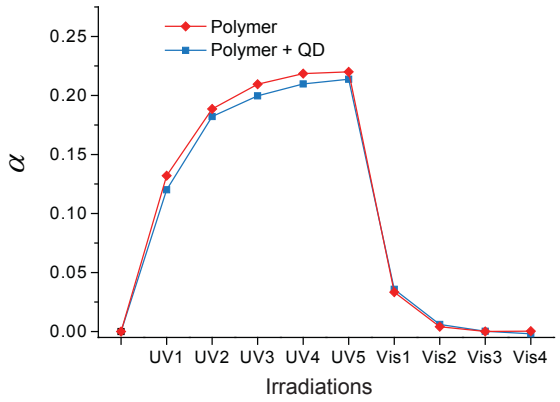


**Supplementary Figure 1:** Change in conversion as a function of irradiation of a THF solution containing either photoswitchable polymer (red) or photoswitchable polymer and QDs (blue). Each point was measured after 60 s of indicated irradiation (UV: 340 nm, 1 mW $cm^{-2}$; Vis: 545 nm, 4.3 mW $cm^{-2}$). A polymer solution of PMA 4PCaoc 75C12 (1.1 mg/ml) in THF was split into two fractions, one of which contained QDs at a final concentration of 90 nM. Both solutions were irradiated first with UV and then with visible light. Photochromic polymers bound to QDs have a lower $\alpha_{PS}$; this phenomenon is not observed in organic solvents. Using the parameters presented in Díaz et al. [1] the $\alpha_{PS}$ of the QD solution should have been ~0.14 if the polymer was bound to the QD. The observed $\alpha_{PS}$ in the presence of QDs was 0.21, very close to the reference value of 0.22, demonstrating a preferential interaction of the polymer cap and of the QDs with the solvent. That is, the polymer existed as a freely draining, dynamic chain in both test solutions.

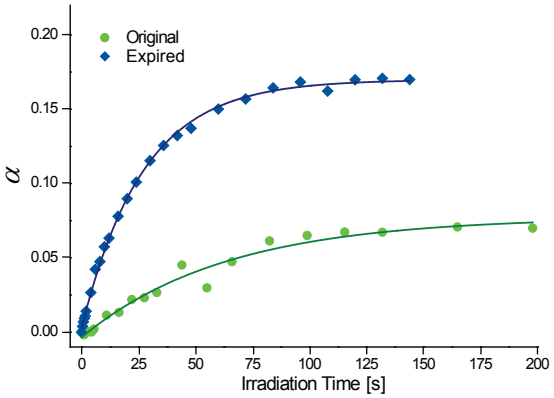


**Supplementary Figure 2:** Photoconversion as a function of UV irradiation time of a solution of psQDs in SBB prepared either with the original QD (QY of psQD, 0.20) or an expired QD (QY of psQD, 0.03). Irradiation at 340 nm (1 mW $cm^{-2}$). The psQDs were prepared with the polymer PMA 8PCaoc 75C12, differing only in the QD selected for coating. The graph demonstrates the differences in photoconversion kinetics and final PS state ($\alpha_{PS}$). The values of $k'_{oc}$ (fits, solid lines) were 0.019±0.001 $s^{-1}$ and 0.037±0.001 $s^{-1}$ for the original and expired QDs, respectively. The lower QY of the expired QDs led to a decrease in $R_o$ (by 1/3) and thus also in the extent of cPC backconversion, causing $\alpha_{PS}$ to increase from 0.07 to 0.17.

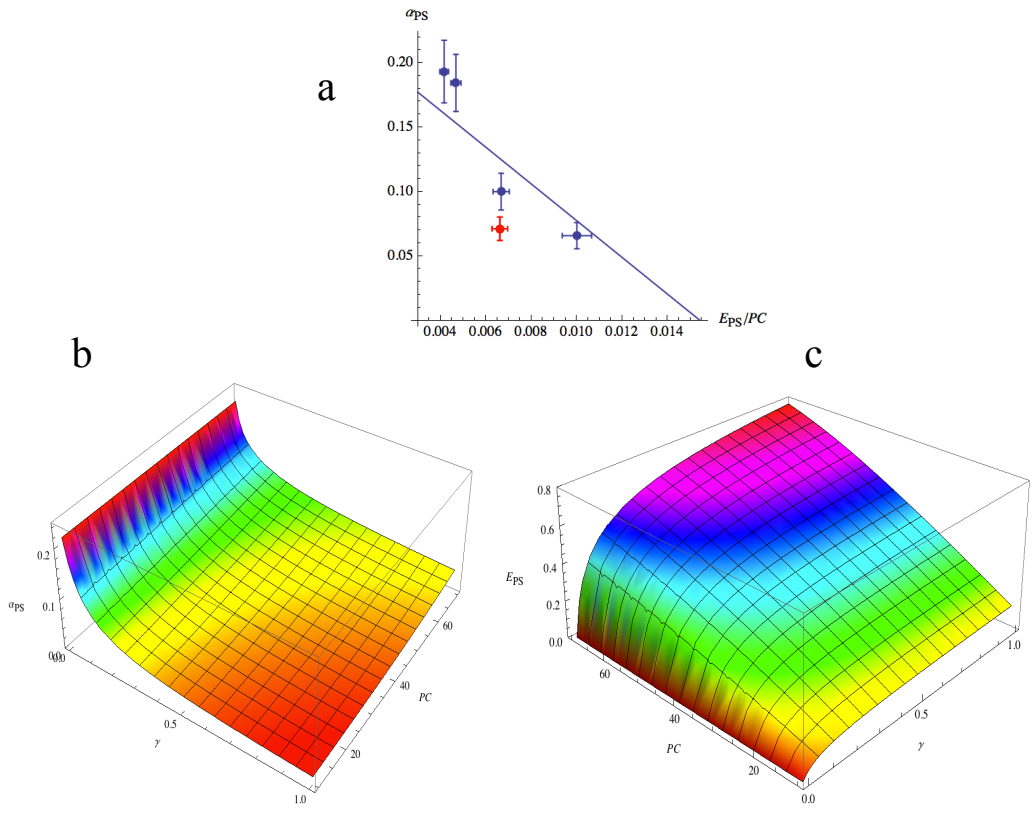


**Supplementary Figure 3**: Partial conformity of the five psQD species in the PS state with the single-component pcFRET mechanism. a) Representation according to Equation 2 of data of Fig. 2. The red point, corresponding to psQD class 5 ($PCadoNH_2$), was not included in the linear regression (see text). Simulations of dependency of $\alpha_{PS}$ (b) and $E_{PS}$ (c) on $PC$ and $\gamma$, according to Supplementary Equations 3 and 4. See text for discussion.

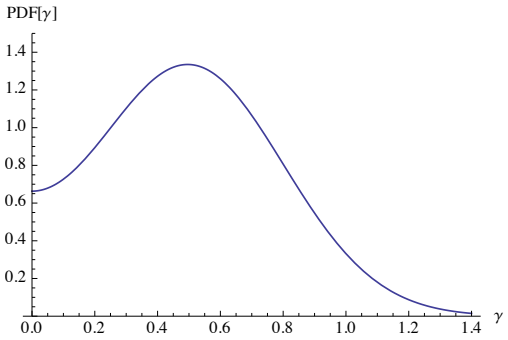


**Supplementary Figure 4**: Probability density function of a simulated population of 12 species with $PC_i$ given by $50 \cdot \int_{\gamma}^{\gamma+\Delta\gamma} \mathrm{PDF}[\gamma]$ in successive $\gamma$ segments 0.117 in width ($\Delta\gamma$).

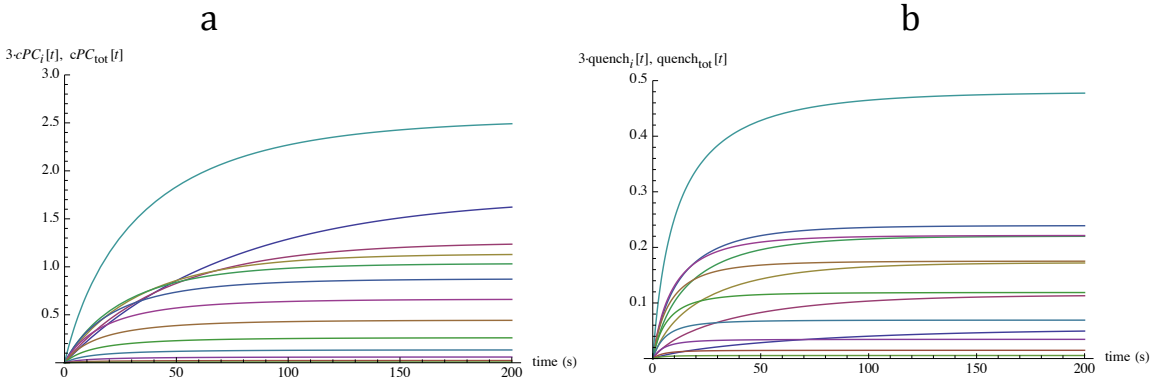


**Supplementary Figure 5**: Time course of cyclization of species defined in Supplementary Figure 4 according to Eqs. 1 and 2, using $k_1 = 0.002$, $k_2 = 3.545\ k_1$, and $k_3 = 80 \cdot k_1$ (units $s^{1}$). a) $cPC[t]$. b) quench$[t]$. The highest curve in each panel corresponds to the total signals; the individual signals are shown expanded 3-fold.

## psQD $PCmNH_2$

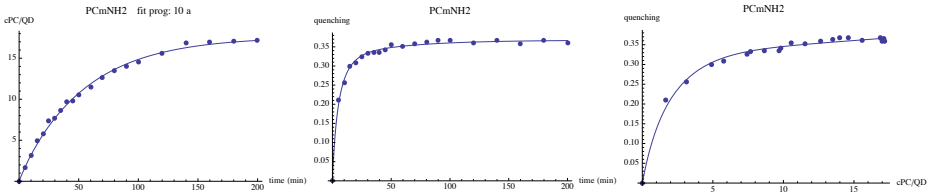


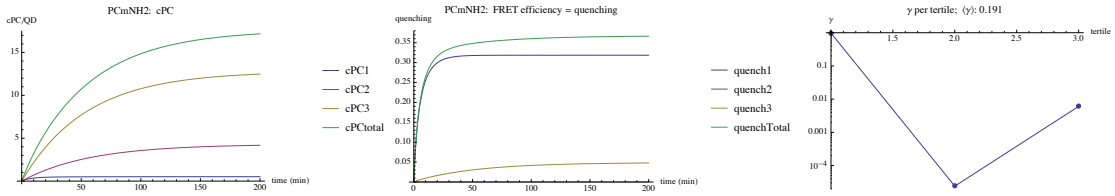


$\{c1 \to 0.00389079, c3 \to 0.205201, \gamma 1 \to 0.975475, \gamma 2 \to 0.000023991, \gamma 3 \to 0.00603627, n1 \to 19.1477, n2 \to -19.552, nn \to 1.39435\}$
$R^2$: 0.999518
[err/val]: c1: 0.015; c3: 0.041; γ1: 0.010; γ2: 419.880; γ3: 0.713; n1: 0.009; n2: 0.006; n3: 0.003
PC in 3 clsses (n1,n2,n3,ntot): {19.1477, 19.552, 60.7659, 99.4656}
Photostationary state --- cPC: {0.515381, 4.176, 12.4812}
αps: {0.0269161, 0.213584, 0.205398}
quenching: {0.318557, 0.0000634821, 0.0477384}
γ: {0.975475, 0.000023991, 0.00603627}
⟨γ⟩: 0.191±0.004
⟨γps⟩: 0.034
kt/kd = cPC[[i]]·γ[[i]]: {0.502741, 0.000100186, 0.0753399}
c1: 0.00389079; c3: 0.205201
c3/c1: nf1[52.7403]±nf1[2.29432]
γ1/γ1x: 0.975475; γ2/γ2x: 0.0023991; γ3/γ3x: 6.03627
n1/n1x: 0.8641; n2/n2x: 0.661761; ntot/ntotx: 1.12218

## psQD $PCalaNH_2$

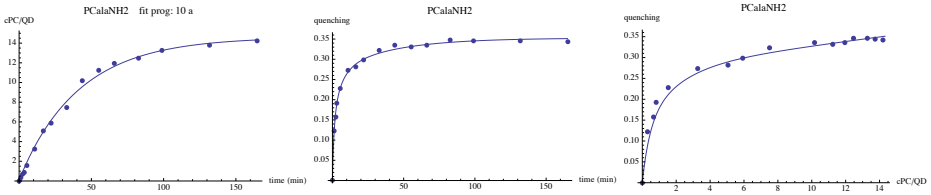


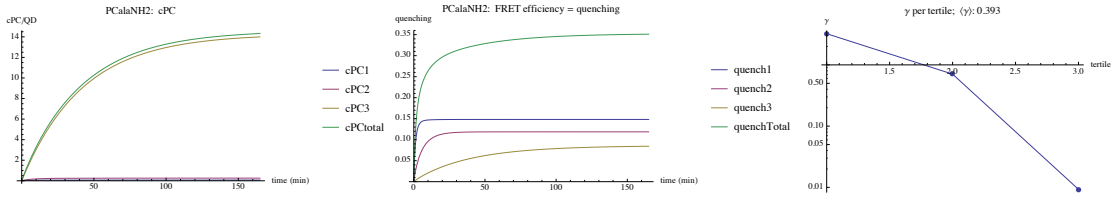


$\{c1 \to 0.0049157, c3 \to 0.272936, \gamma 1 \to 3.23012, \gamma 2 \to 0.706579, \gamma 3 \to -0.00928742, n1 \to 8.54787, n2 \to 7.7655, nn \to 1.8365\}$
$R^2$: 0.999058
[err/val]: c1: 0.029; c3: 0.068; γ1: 0.009; γ2: 0.057; γ3: 0.165; n1: 0.026; n2: 0.035; n3: 0.005
PC in 3 clsses (n1,n2,n3,ntot): {8.54787, 7.7655, 69.6435, 85.9569}
Photostationary state --- cPC: {0.0706835, 0.258737, 13.9949}
αps: {0.00827994, 0.0333627, 0.20322}
quenching: {0.14815, 0.118628, 0.0843395}
γ: {3.23012, 0.706579, 0.00928742}
⟨γ⟩: 0.393±0.010
⟨γps⟩: 0.038
kt/kd = cPC[[i]]·γ[[i]]: {0.228316, 0.182818, 0.129976}
c1: 0.0049157; c3: 0.272936
c3/c1: nf1[55.5234]±nf1[4.11583]
γ1/γ1x: 6.46024; γ2/γ2x: 706.579; γ3/γ3x: 928.742
n1/n1x: 1.10619; n2/n2x: 1.00495; ntot/ntotx: 1.11238

## psQD PCahxNH$_2$

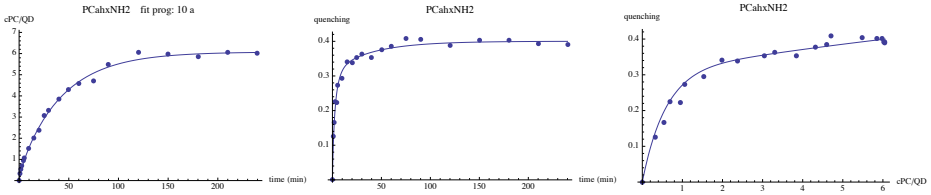


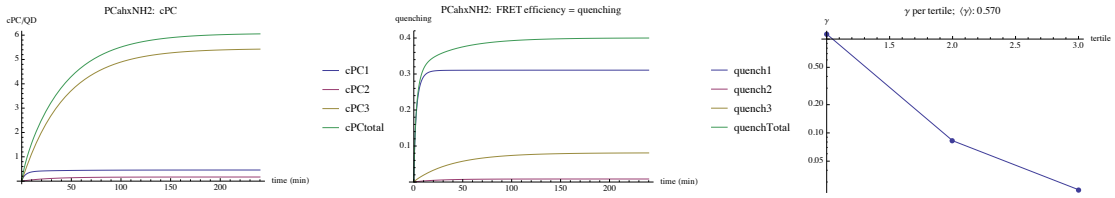


$\{c1 \to 0.00386184, c3 \to 0.38944, \gamma1 \to -1.13148, \gamma2 \to 0.082634, \gamma3 \to 0.0248261, n1 \to 33.4128, n2 \to 1.62018, nn \to 1.49732\}$

$R^2$: 0.998789

[err/val]: c1: 0.020; c3: 0.027; γ1: 0.007; γ2: 0.093; γ3: 0.093; n1: 0.011; n2: 0.005; n3: 0.011

PC in 3 clsses (n1,n2,n3,ntot): {33.4128, 1.62018, 32.9454, 67.9784}

Photostationary state --- cPC: {0.457604, 0.169642, 5.42551}

αps: {0.0136631, 0.104204, 0.161542}

quenching: {0.310697, 0.00841184, 0.0808254}

γ: {1.13148, 0.082634, 0.0248261}

⟨γ⟩: 0.570±0.008

⟨γps⟩: 0.110

kt/kd = cPC[[i]]·γ[[i]]: {0.51777, 0.0140182, 0.134694}

c1: 0.00386184; c3: 0.38944

c3/c1: nf1[100.843]±nf1[3.3351]

γ1/γ1x: 0.377161; γ2/γ2x: 0.82634; γ3/γ3x: 24.8261

n1/n1x: 1.67064; n2/n2x: 0.162018; ntot/ntotx: 1.13297

## psQD PCaocNH$_2$

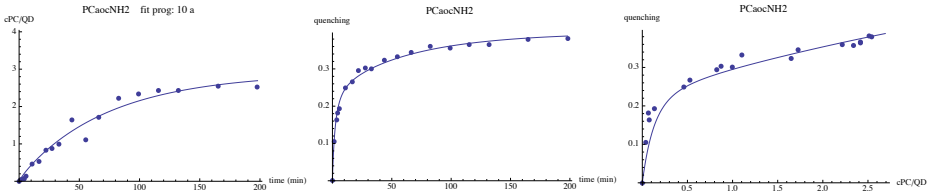


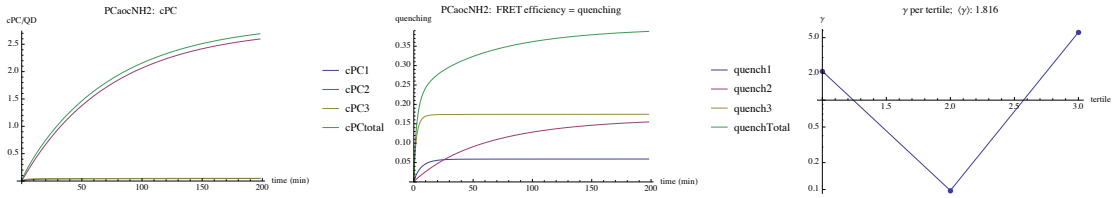


$\{c1 \to 0.00186223, c3 \to 0.0929649, \gamma1 \to 2.10267, \gamma2 \to -0.0974093, \gamma3 \to 5.74503, n1 \to 3.16105, n2 \to 20.9662, nn \to -1.94027\}$

$R^2$: 0.992954

[err/val]: c1: 0.066; c3: 0.112; γ1: 0.025; γ2: 0.181; γ3: 0.014; n1: 0.035; n2: 0.050; n3: 0.118

PC in 3 clsses (n1,n2,n3,ntot): {3.16105, 20.9662, 8.93742, 33.0647}

Photostationary state --- cPC: {0.0458891, 2.59632, 0.049616}

αps: {0.0146198, 0.127988, 0.00558984}

quenching: {0.0590351, 0.154735, 0.174399}

γ: {2.10267, 0.0974093, 5.74503}

⟨γ⟩: 1.816±0.202

⟨γps⟩: 0.236

kt/kd = cPC[[i]]·γ[[i]]: {0.0964894, 0.252906, 0.285046}

c1: 0.00186223; c3: 0.0929649

c3/c1: nf1[49.9213]±nf1[6.49862]

γ1/γ1x: 2.10267; γ2/γ2x: 3.24698; γ3/γ3x: 5745.03

n1/n1x: 0.105368; n2/n2x: 2.09662; ntot/ntotx: 0.876413

psQD PCadoNH$_2$

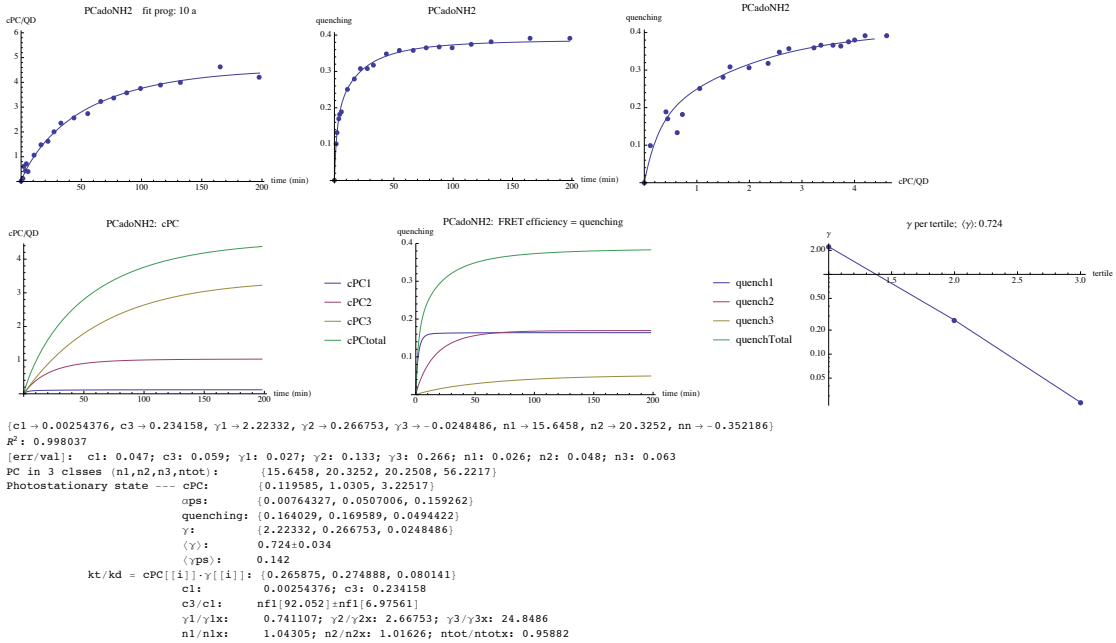


```
{c1 → 0.00254376, c3 → 0.234158, γ1 → 2.22332, γ2 → 0.266753, γ3 → -0.0248486, n1 → 15.6458, n2 → 20.3252, nn → -0.352186}
R²: 0.998037
[err/val]:  c1: 0.047; c3: 0.059; γ1: 0.027; γ2: 0.133; γ3: 0.266; n1: 0.026; n2: 0.048; n3: 0.063
PC in 3 clsses (n1,n2,n3,ntot):      {15.6458, 20.3252, 20.2508, 56.2217}
Photostationary state --- cPC:       {0.119585, 1.0305, 3.22517}
                          αps:       {0.00764327, 0.0507006, 0.159262}
                          quenching: {0.164029, 0.169589, 0.0494422}
                          γ:         {2.22332, 0.266753, 0.0248486}
                          ⟨γ⟩:       0.724±0.034
                          ⟨γps⟩:     0.142
                kt/kd = cPC[[i]]·γ[[i]]: {0.265875, 0.274888, 0.080141}
                          c1:         0.00254376; c3: 0.234158
                          c3/c1:      nf1[92.052]±nf1[6.97561]
                          γ1/γ1x:     0.741107; γ2/γ2x: 2.66753; γ3/γ3x: 24.8486
                          n1/n1x:     1.04305; n2/n2x: 1.01626; ntot/ntotx: 0.95882
```

**Supplementary Figure 6**: Fits to psQD data of Figs. 2d,e,f according to Eqs. 1 and 2. The fit parameters are indicated with each data set. The parameters c1, c2, and c3 correspond to $k_1$, $k_2$, $k_3$ in Equation (1), and n = n1 + n2 + n3 to $PC = PC_1+PC_2+PC_3$. First row of images (left to right): experimental quantities and corresponding fits. Second row of images (left to right): calculated values of $cPC_{1,2,3}$, $E_{1,2,3}$, and $\gamma_{1,2,3}$ ; kt/kd = $k_{t,i}/k_{d,o}$ Relative fit errors (s.e./val) and various numerical values for given calculated quantities follow. See text and Supplementary Note 3 for detailed explanation. The fit parameters are also given in Supplementary Table 2.

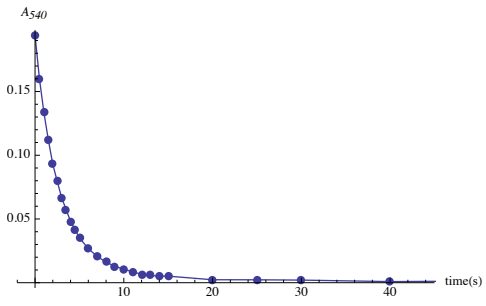


**Supplementary Figure 7**: Cycloreversion kinetics of psQD PCalaNH$_2$ monitored by absorption. The sample (0.46 $\mu$M) was first taken to the PS state by UV irradiation and then exposed to visible light at 550 nm (8.2 mW cm$^{-2}$). The monoxponential analysis yielded $k'_{co}$ = 0.35±0.01 s$^{-1}$. The reaction monitored by the increase in QD fluorescence (56%) gave $k'_{co}$ = 0.37±0.04 s$^{-1}$.

**Supplementary Table 1**: Fluorescence lifetimes of the psQDs

| psQD | $\langle\tau_{amp}\rangle$ [ns] | $\Delta\langle\tau_{amp}\rangle$ |
|---|---|---|
| $PCmNH_2$ | 3.4±0.1 | 32±4 |
| $PCalaNH_2$ | 3.9±0.1 | 31±4 |
| $PCahxNH_2$ | 6.4±0.3 | 35±6 |
| $PCaocNH_2$ | 6.5±0.2 | 37±4 |
| $PCadoNH_2$ | 4.7±0.2 | 35±5 |
| psQR | 14.8±0.4 | 14±2 |

Fluorescence lifetime measurements were performed in a Fluoro-Log-TCSPC spectrofluorimeter (Horiba Jobin Yvon). The excitation was carried out with a nanoLED N-320, and the emission monochromator was set to the peak at 550 nm. Other conditions:, TAC range, 500 ns; pulse repetition frequency, 500 kHz; and 10,000 counts peak value for automatic timing. The amplitude weighted mean lifetime, $\langle\tau_{amp}\rangle$, was determined from 3-4 exponential components determined with fitting programs implemented with *Mathematica* 8.0 (Wolfram Research).

**Supplementary Table 2**: Tabulated parameters derived from the fits in Supplementary Figure 6.

| psQD | $10^3 \cdot k_1$ [s$^{-1}$] | $k_3$ [s$^{-1}$] | $k_3/k_1$ | $\gamma_1$ | $\gamma_2$ | $\gamma_3$ | $\langle\gamma\rangle$ |
|---|---|---|---|---|---|---|---|
| $PCmNH_2$ | 3.9 (0.01) | 0.20 (0.04) | 53±2 | 0.98 (0.01) | $<10^{-4}$ | 0.006 (0.7) | 0.191 (0.004) |
| $PCalaNH_2$ | 4.9 (0.03) | 0.27 (0.07) | 56±4 | 3.23 (0.01) | 0.70 (0.06) | 0.01 (0.2) | 0.39 (0.01) |
| $PCahxNH_2$ | 3.9 (0.02) | 0.39 (0.03) | 101±3 | 1.13 (0.01) | 0.08 (0.09) | 0.03 (0.09) | 0.57 (0.01) |
| $PCaocNH_2$ | 1.9 (0.07) | 0.09 (0.11) | 50±7 | 2.10 (0.03) | 0.10 (0.20) | 5.8 (0.01) | 1.8 (0.2) |
| $PCadoNH_2$ | 2.5 (0.05) | 0.23 (0.06) | 92±7 | 2.22 (0.03) | 0.27 (0.13) | 0.03 (0.3) | 0.72 (0.03) |

| psQD | $n_1$ | $n_2$ | $n_3$ | $n_{tot}$ | $cPC_1$ | $cPC_2$ | $cPC_3$ | $cPC_{tot}$ |
|---|---|---|---|---|---|---|---|---|
| $PCmNH_2$ | 19.1 (0.01) | 19.6 (0.006) | 60.8 | 99 | 0.52 | 4.2 | 12.5 | 17.2 |
| $PCalaNH_2$ | 8.5 (0.03) | 7.7 (0.04) | 69.6 | 86 | 0.071 | 0.26 | 14 | 14.3 |
| $PCahxNH_2$ | 33.4 (0.01) | 1.6 (0.01) | 32.9 | 68 | 0.46 | 0.17 | 5.4 | 6.1 |
| $PCaocNH_2$ | 3.2 (0.04) | 21 (0.05) | 8.9 | 33 | 0.046 | 2.6 | 0.05 | 2.7 |
| $PCadoNH_2$ | 15.6 (0.03) | 20.3 (0.05) | 20.2 | 56 | 0.12 | 1.03 | 3.2 | 4.4 |

| psQD | $\alpha_{PS,1}$ | $\alpha_{PS,2}$ | $\alpha_{PS,3}$ | $\alpha_{PS,tot}$ | $quench_1$ | $quench_2$ | $quench_3$ | $quench_{tot}$ |
|---|---|---|---|---|---|---|---|---|
| $PCmNH_2$ | 0.027 | 0.213 | 0.205 | 0.173 | 0.319 | $<10^{-4}$ | 0.048 | 0.367 |
| $PCalaNH_2$ | 0.008 | 0.033 | 0.203 | 0.166 | 0.148 | 0.119 | 0.084 | 0.351 |
| $PCahxNH_2$ | 0.014 | 0.105 | 0.165 | 0.089 | 0.311 | 0.008 | 0.081 | 0.4 |
| $PCaocNH_2$ | 0.015 | 0.124 | 0.006 | 0.082 | 0.059 | 0.155 | 0.174 | 0.388 |
| $PCadoNH_2$ | 0.008 | 0.051 | 0.159 | 0.078 | 0.164 | 0.17 | 0.049 | 0.383 |

| psQD | $k_{t,1}/k_{d,0}$ | $k_{t,2}/k_{d,0}$ | $k_{t,3}/k_{d,0}$ | $k_{t,tot}/k_{d,0}$ | $R^2$ |
|---|---|---|---|---|---|
| $PCmNH_2$ | 0.502 | $<10^{-5}$ | 0.075 | 0.577 | 0.999 |
| $PCalaNH_2$ | 0.228 | 0.183 | 0.13 | 0.541 | 0.999 |
| $PCahxNH_2$ | 0.518 | 0.014 | 0.135 | 0.667 | 0.999 |
| $PCaocNH_2$ | 0.096 | 0.253 | 0.285 | 0.634 | 0.993 |
| $PCadoNH_2$ | 0.266 | 0.275 | 0.08 | 0.621 | 0.998 |

$n_{tot} = n_1 + n_2 + n_3$; $R^2$, fit statistic. Quantities in parentheses are relative errors (s.e/value); absolute errors (s.e.) are preceded by "±". $k_2/k_1 = \alpha_{PS,0}^{-1} - 1 = 3.545$.

## Supplementary Note 1: Calculation of FRET Orientation Factor $\kappa^2$

Most treatments of QDs as FRET donors (*D*) and surface acceptors regard the orientation of the latter as sufficiently random and dynamic such that a FRET orientation factor $\kappa^2$ = 2/3 can be assumed. However, this value requires that both *D* and the acceptor *A* reorient during the excited state, a condition that obviously cannot hold for the QD component of the pcFRET system, as well as in many cases for the acceptor.

We assume that the donor excitation can be modeled as being centrosymmetric about the nanocrystal center,[2] and that sucessive QD emissions are random with repect to the donor dipole orientation. In the psQD linker series, the polymer-coupled cPC acceptors are distributed in a concentric shell (or shells), inserted in the matrix of alkyl chains bound to the nanoparticle and to the polymer cap, with their absorption transition moment in some defined orientation with respect to the D-A separation vector (a radius $\vec{R}$) directed to the QD center. $\kappa^2$ is given by $\kappa^2 = (cos[\theta_T] - 3cos[\theta_D]cos[\theta_A])^2$ in which $\theta_T$ is the angle between the *D* and *A* transition moments (emission and absorption, respectively) and $\theta_D$ and $\theta_A$ are the angles between *D* and $\vec{R}$ and *A* and $\vec{R}$, respectively [3]. We identify two extreme cases:

(1) the acceptor oriented along $\vec{R}$ such that $\theta_A = 0$ and $\theta_D = \theta_T$. In this case, $\kappa^2 = 4cos[\theta_T]^2$, the maximal possible value;

(2) the acceptor oriented perpendicular to $\vec{R}$ such that $\theta_A = \pi/2$. In this case, $\kappa^2 = cos[\theta_T]^2$, the minimal possible value.

We now consider the distribution of acceptors (case 1) for a differential angular increment $d\theta_T$. Rotating the *D*-*R* plane about the *D* axis by 360° (2π) defines a spherical zone of FRET-equivalent acceptors. The incremental surface (*dS*) is given by $dS[\theta_T] = 2\pi r \cdot sin[\theta_T] r\theta_T$, where *r* is the radius of the sphere and $2\pi r$ is the circumference of the intersection circle defined by rotating $\vec{R}$. The fraction of acceptors in $dS$ is given by $dS/(2\pi r^2)$. We restrict $\theta_T$ to the range 0-π/2 and thus define a hemisphere. It follows that $\langle\kappa^2\rangle$ for a population of acceptors, randomly located in the spherical shell (the two hemispheres are equivalent), is given by:

$$\langle\kappa^2\rangle = \frac{2}{\pi}\int_0^{\pi/2} \frac{\kappa^2[\theta_T]}{2\pi r^2} dS[\theta_T] = \frac{8}{\pi}\int_0^{\pi/2} cos[\theta_T]^2 \, sin[\theta_T] d\theta_T = \frac{8}{3\pi} = 0.849 \qquad (1)$$

$R^6_{0,-\kappa^2} = c_o J n^{-4} Q = 4.1^6$ nm$^6$ was computed with the following parameters: $c_o = 8.8 \cdot 10^{-28}$; $J = 1.3 \cdot 10^{32}$; $n = 1.47$; and $Q = 0.20$.

## Supplementary Note 2: Photostationary State of Unimodal psQDs

The systematically controlled spatial distribution of acceptors is a new feature requiring a more detailed formalism in order to derive quantitative interpretations of experimental data. The PS state is defined by setting the derivative given in Eq. 1 to zero, which after substitution and rearrangement leads to an expression establishing a linear relationship between $\alpha_{\mathrm{PS}}$ and $E_{\mathrm{PS}}/PC$.

$$\alpha_{\mathrm{PS},j} = \frac{1-(k_3/k_1)\cdot E_{t,\mathrm{PS},j}/PC_j}{1-k_2/k_1} = \alpha_{\mathrm{PS},0}\left[1-(k_3/k_1)\cdot E_{\mathrm{PS},j}/PC_j\right] \qquad (2)$$

in which the terms are defined as in Eq. 1; $j$ is an index for the 5 classes of psQDs. A test of the consistency of Supplementary Equation 2 with the experimental data ($E_{\mathrm{PS}}$, $PC$ and $\alpha_{\mathrm{PS}}$ from Tables 1,2) is given in Supplementary Figure 3a; the linear regression yields $k_3/k_1$ = 72±11, from which we calculate the ratio of the forward and reverse photoconversion quantum yields, $\Phi_{\mathrm{co}}/\Phi_{\mathrm{oc}} = 0.42 \pm 0.06$. A somewhat different value (0.78) for the same quantity was derived from $k_2/k_1 = \alpha_{\mathrm{PS},0}^{-1} - 1 = 3.545$. We further tested Supplementary Equation 2 by using our previously reported data[4] of a psQD irradiated at a different UV wavelength (365 nm). The increase in $k_2/k_1$ (2.9-fold) and $k_3/k_1$ (2.4-fold) correlated with a lower $\alpha_{\mathrm{PS}}$ (reduced by 2/3) and $E_{\mathrm{PS}}$ (0.2).

Analytical expressions for $\alpha_{\mathrm{PS}}$ and $E_{\mathrm{PS}}$ as function of PC and $\gamma$ can also be derived (Supplementary Equations 3 and 4), leading to the 3D plots shown in Supplementary Figures 3,b,c. It is interesting that increasing $\gamma$ drives $\alpha_{\mathrm{PS}}$ towards 0 (red region) or to a finite limiting value (yellow region), depending on whether the value of $PC$ is less or greater than $k_3/k_1$, respectively. For the latter case, $\alpha_{\mathrm{PS},\gamma\to\infty}$ is given by Equation 2 evaluated for $E_{\mathrm{PS}}$ = 1. In contrast, $E_{\mathrm{PS}}$ always increases as a function of $\gamma$ and $PC$. A fairly good approximation is given by $E_{\mathrm{PS}}[\gamma] \cong PC\ \alpha_{\mathrm{PS},0}\gamma/\left[1+\ (k_3/k_1)\alpha_{\mathrm{PS},0}\gamma\right]$, with a limit at high $\gamma$ values equal to $PC(k_1/k_3)$. Supplementary Figure 3c demonstrates "bands" of relative constant $E_{\mathrm{PS}}$ defined by reciprocal ("low-high", "high-low) combinations of $PC$ and $\gamma$. However, the formalism is unable to account for the constancy of $E_{\mathrm{PS}}$ exhibited by the psQDs with different linker lengths.

$$\alpha_{\mathrm{PS}}[\gamma\_]:= \left(x = 1 + k_2/k_1 + (k_3/k_1 - PC)\gamma; y = (1+k_2/k_1)PC\cdot\gamma; \frac{\sqrt{x^2+4y}-x}{2y}\right) \qquad (3)$$

$$E_{\mathrm{PS}}[\gamma\_]:= \left(\frac{PC\cdot\gamma}{1+k_2/k_1}; y = \frac{(k_3/k_1-PC)\gamma}{1+k_2/k_1};\ z = \sqrt{4x+(1+y)^2} - y; \frac{z-1}{z+1}\right) \qquad (4)$$

## Supplementary Note 3: Data fitting and Derived Parameters

Fitting the data with Eqs. 1 and 2 was performed with the *Mathematica* function *ParametricNDSolveValue* for solving sets of differential equations and associated time dependent non-differential equations as functions of parameters optimized by *NonlinearModelFit*. In this way error values for all the fitted parameters were obtained. For joint fitting of the *cPC*[*t*] and quench[*t*] data, the vectors were catenated and the *cPC*[*t*] values scaled so as to correspond numerically to the quenching data (given in fractional units). The *cPC*[*t*] values were assigned a relative weight of 1.5, a condition that provided greater consistency to the fits. The known photostationary state was imposed by the condition $k_2 = 3.545 \cdot k_1$. The fit parameters are described in the text.

Before showing the fits to the experimental data, a simulation is presented of a model system consisting of 12 subspecies, with the $PC_i$ distributed in a discretized manner according to the probability density function (PDF) shown in Supplementary Figure 4. The time course of the respective $cPC_i[t]$, the total *cPC*[*t*] and the corresponding quench[*t*] signals are given in Supplementary Figures 5b and 5c, respectively. In order of increasing $\gamma$, $cPC_i[t]$ decreased in velocity and attained a higher end value. In the case of $\text{quench}_i[t]$, increasing $\gamma$ led to greater reaction velocities and higher end values. Some of the curve crossings apparent in Supplementary Figure 5 are due to the nature of the PDF function selected for the simulation.

The fits to the experimental *cPC* and *E* data of the 5 classes of psQDs are shown in Supplementary Figure 6 and Supplementary Table 2, and a representative cycloreversion reaction in Supplementary Figure 7.

# Supplementary Methods

## Synthesis of psQDs

### 3-(3,3,4,4,5,5-hexafluoro-2-(2-methylbenzo[b]thiophen-3-yl)cyclopent-1-enyl)-2-methylbenzo[b]thiophen-6-amine

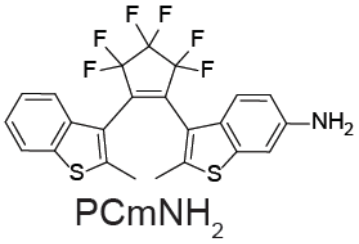


A solution of $PCmNO_2$ (3-(3,3,4,4,5,5-hexafluoro-2-(2-methylbenzo[b]thiophen-3-yl)cyclopent-1-enyl)-2-methyl-benzo-[b]thiophen-6-amine; 24 mg, 46.7 µmol) was prepared in 5 mL of methanol. $NiCl_2 \cdot 6H_2O$ (86.76 mg) was added under vigorous mixing until complete solubility of $PCmNO_2$ was achieved. The solution was placed in an ice bath, and then $NaBH_4$ (43.5 mg, 1.14 mmoles) was added slowly, leading to the immediate formation of a black precipitate. The solution reached completion in ~10 min at RT, was quenched with 0.04 N HCl, filtered, and then evaporated in a rotovap. The residue was extracted with $CH_2Cl_2$, and the organic phase was washed with water, dried with $Na_2SO_4$, filtered, and evaporated in a rotovap. Purification was realized on a silica column (100% cyclohexane with gradual increase of ethyl acetate until 90:10 is reached). $PCmNH_2$ was obtained as a pink oil ($R_f$ = 0.25, 70:30 cyclohexane: ethyl acetate; 16.9 mg, yield: 75%).$^1$H NMR (400MHz, $CDCl_3$) δ 2.10 (s, 2.9H, CH3 ap), 2.21 (s, 3.1H, CH3 ap) 2.43 (2s, 3.3H, CH3 p), 6.54 (d, 0.4H, H-5 p), 6.77 (d, 0.9H, H-5 ap), 6.87 (s, 0.4H, H-7 p), 6.96 (s, 0.8H, H-7 ap), 7.17-7.77 (m, 9.5H, ArH). [p:ap] conformers, 35:65.

## Acyl Chlorides

A commercially available linker which presented a carboxyl group on one end and a protected amine on the other (205 µmol) was added to a flask that had been previously dried and flushed with argon. Thionyl chloride (22 µl, 300 µmol, CAS: 7719-09-7) was added, the flask was flushed with argon and the reaction allowed to proceed for 30 min at 50 ºC. The flask was dried in a rotovap for 60 min at 50 ºC. Excess reagent, $SO_2$, and HCl were eliminated and freshly formed acyl chloride used in the next step.

### 2-amino-N-(3-(3,3,4,4,5,5-hexafluoro-2-(2-methylbenzo[b]thiophen-3-yl)cyclopent-1-enyl)-2-methylbenzo[b]thiophen-6-yl)propanamide

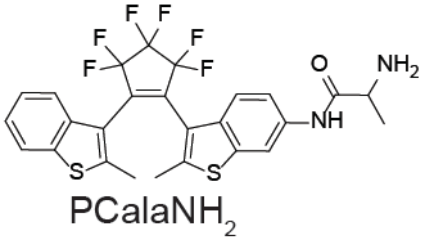


A solution containing $PCmNH_2$ (48 mg, 100 µmol) was dissolved in dry $CHCl_3$. The solution was added to a dry flask containing (9H-fluoren-9-yl)methyl-1-chloro-1-oxopropan-2-ylcarbamate (59 mg, 180 µmol) and allowed to react at 30 ºC for 2 h. The reaction was

neutralized with NaOH and the crude product was extracted with $CH_2Cl_2$; a pink oil was obtained. Purification was performed on a silica gel column with cyclohexane: ethyl acetate (70:30) mobile phase. The intermediate product (9H-fluoren-9-yl)methyl 1-(3-(3,3,4,4,5,5-hexafluoro-2-(2-methylbenzo[b]thiophen-3-yl)cyclopent-1-enyl)-2-methylbenzo[b]thiophen-6-ylamino)-1-oxopropan-2-yl carbamate, PcalaFmoc, was obtained (64 mg, 84 µmol) as a red foam. ($R_f$ = 0.30, 70:30 cyclohexane: ethyl acetate)

The Fmoc protective group was released from the aliphatic amine by addition of excess piperidine (650 µl, 6.5 mmoles) in $CHCl_3$ at 50 ºC for 20 min. The reaction was quenched with HCl and extracted with $CH_2Cl_2$. The product was purified by silica gel column, with cyclohexane: THF (30:70) mobile phase. The solvent was evaporated in a rotovap and the final product was obtained as a yellow/brown oil ($R_f$ = 0.0, 70:30 cyclohexane: ethyl acetate; 41.5 mg, yield: 75%). $^1$H NMR (400 MHz, $CDCl_3$) δ 1.27 (d*,* 1.05H, CH3 p), 1.29 (s*,* 1.25H, CH3), 2.17 (*s,* 1.20H, Ar-CH3 ap), 2.20 (s, 1.75H, Ar-CH3 ap), 2.48 (2*s,* 2.40H, Ar-CH3 p), 3.65 (m, 1.07, CH), 6.80-7.70 (m, 6H, ArH), 8.31 (*s,* 0.40H, H-7 ap), 8.35 (*s,* 0.20H, H-7 p), 9.53 (s, 0.30H, Ar-NH-CO), 9.65 (s, 0.51H, Ar-NH-CO). [p:ap] conformers, 40:60.

**6-amino-N-(3-(3,3,4,4,5,5-hexafluoro-2-(2-methylbenzo[b]thiophen-3-yl)cyclopent-1-enyl)-2-methylbenzo[b]thiophen-6-yl)hexanamide**

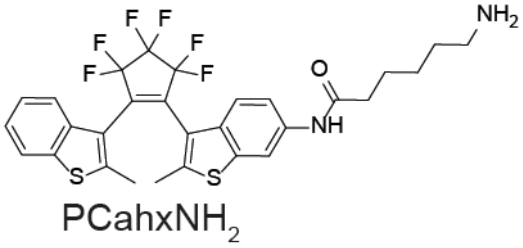

PCahxNH$_2$

A solution containing PCmNH$_2$ (48 mg, 100 µmol) was dissolved in dry $CHCl_3$. The solution was added to a dry flask containing tert-butyl 6-chloro-6-oxohexylcarbamate (45 mg, 180 µmol) and allowed to react at 30 ºC for 2 h. The reaction was neutralized with NaOH solution and the crude was extracted with $CH_2Cl_2$; a greenish-brownish oil was obtained. Purification was performed on a silica gel column with cyclohexane:ethyl acetate (90:10) mobile phase. The intermediate product tert-butyl 6-(3-(3,3,4,4,5,5-hexafluoro-2-(2-methylbenzo[b]thiophen-3-yl)cyclopent-1-enyl)-2 methylbenzo[b]thiophen-6-ylamino)-6-oxohexylcarbamate was obtained (38 mg, 54.4 µmol) as a pink oil. ($R_f$ = 0.55, 50:50 cyclohexane: ethyl acetate)

The BOC protective group was released from the aliphatic amine by addition of 20% fuming HCl in ethyl acetate for 10 min at RT. The reaction was quenched with NaOH and extracted with $CH_2Cl_2$. The product was purified over a silica gel filter; impurities were removed with washes of cyclohexane: ethyl acetate (from 100% cyclohexane to 100% ethyl acetate) and then the product was obtained by eluting with DMF. Solvent was evaporated in a rotovap and the final product was obtained as a pink/orange oil ($R_f$ = 0.0, 70:30 cyclohexane: ethyl acetate; 20 mg, yield: 33%). $^1$H NMR (400 MHz, $CDCl_3$) δ 1.25 (m*, 1.*94H, CH2-CH2-CH2), 1.51 (m*, 2.*30H, CH2), 1.72 (m*, 2.*07H, CH2), 2.13 (*s,* 1.20H, CH3

ap), 2.16 (s, 1.18H, CH3 ap), 2.34 (t, *2*.04H, NH-CO-CH2), 2.43 (2*s,* 2.66H, CH3 p), 2.71 (m, *2*.00H, CH2-NH2), 6.85-7.70 (m, 6H, ArH), 8.18 (*s,* 0.35H, H-7 p), 8.22 (*s,* 0.65H, H-7 ap). [p:ap] conformers, 40:60.

**8-amino-N-(3-(3,3,4,4,5,5-hexafluoro-2-(2-methylbenzo[b]thiophen-3-yl)cyclopent-1-enyl)-2-methylbenzo[b]thiophen-6-yl)octanamide**

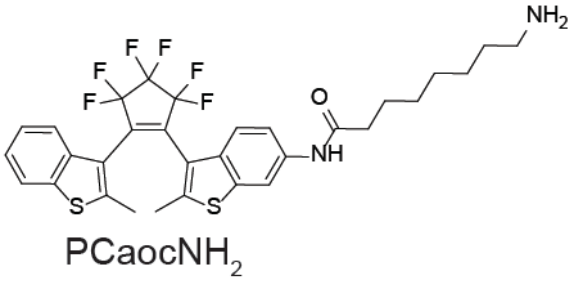

PCaocNH$_2$

A solution containing PCmNH$_2$ (48 mg, 100 µmol) was dissolved in dry $CHCl_3$. The solution was added to a dry flask containing (9H-fluoren-9-yl)methyl 8-chloro-8-oxooctylcarbamate (72.0 mg, 180 µmol) and allowed to react at 30 ºC for 2 h. The reaction was neutralized with NaOH and the crude product was extracted with $CH_2Cl_2$; a pink oil was obtained. Purification was performed on a silica gel column with cyclohexane: ethyl acetate (70:30) mobile phase. The intermediate product (9H-fluoren-9-yl)methyl 8-(3-(3,3,4,4,5,5-hexafluoro-2-(2-methylbenzo[b]thiophen-3-yl)cyclopent-1-enyl)-2-methylbenzo[b]thiophen-6-ylamino)-8-oxooctylcarbamate, PCaocFmoc, was obtained (61.8 mg, 73 µmol) as a pink wax. ($R_f$ = 0.40, 60:40 cyclohexane: ethyl acetate)

The Fmoc protective group was released from the aliphatic amine by addition of excess piperidine (650 µl, 6.5 mmoles) in $CHCl_3$ at 50 ºC for 20 min. The reaction was quenched with HCl and extracted with $CH_2Cl_2$. The product was purified by silica gel column, with cyclohexane: THF (30:70) mobile phase. The solvent was evaporated in a rotovap and the final product was obtained as a pink-yellow oil ($R_f$ = 0.0, 70:30 cyclohexane: ethyl acetate; 27.5 mg, yield: 44%). $^1$H NMR (400 MHz, $CDCl_3$) δ 1.33 (m, *9*.98H, CH2-CH2-CH2), 1.51 (m, *2*.30H, CH2), 1.72 (m, *2*.07H, CH2), 2.13 (*s,* 1.70H, CH3 ap), 2.16 (s, 2.08H, CH3 ap), 2.34 (t, *2*.26H, NH-CO-CH2), 2.43 (2*s,* 2.71H, CH3 p), 2.71 (m, *2*.00H, CH2-NH2), 6.85-7.70 (m, 6H, ArH), 8.18 (*s,* 0.42H, H-7 p), 8.22 (*s,* 0.65H, H-7 ap).
[p:ap] conformers, 40:60.

**12-amino-N-(3-(3,3,4,4,5,5-hexafluoro-2-(2-methylbenzo[b]thiophen-3-yl)cyclopent-1-enyl)-2-methylbenzo[b]thiophen-6-yl)dodecanamide**

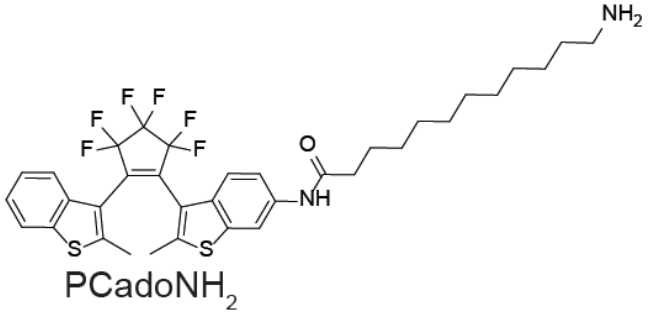

PCadoNH$_2$

A solution containing PCmNH$_2$ (48 mg, 100 µmol) was dissolved in dry $CHCl_3$. The solution was added to a dry flask containing (9H-fluoren-9-yl)methyl 12-chloro-12-oxododecyl-carbamate (82.1 mg, 180 µmol) and allowed to react at 30 ºC for 2 h. The

reaction was neutralized with NaOH and the crude product was extracted with $CH_2Cl_2$; a pink oil was obtained. Purification was performed on a silica gel column with cyclohexane: ethyl acetate (70:30) mobile phase. The intermediate product (9H-fluoren-9-yl)methyl 12-(3-(3,3,4,4,5,5-hexafluoro-2-(2-methylbenzo[b]thiophen-3-yl)cyclopent-1-enyl)-2-methylbenzo[b]thiophen-6-ylamino)-12-oxododecylcarbamate, PCaocFmoc, was obtained (40.6 mg, 45 µmol) as a golden oil. oil ($R_f$ = 0.65, 60:40 cyclohexane: ethyl acetate)

The Fmoc protective group was released from the aliphatic amine by addition of excess piperidine (650 µl, 6.5 mmoles) in $CHCl_3$ at 50 ºC for 20 min. The reaction was quenched with HCl and extracted with $CH_2Cl_2$. The product was purified by silica gel column, with cyclohexane: THF (30:70) mobile phase. The solvent was evaporated in a rotovap and the final product was obtained as a pink-yellow oil ($R_f$ = 0.0, 70:30 cyclohexane: ethyl acetate; 18.3 mg, yield: 27%). $^1$H NMR (400 MHz, $CDCl_3$) δ 1.27 (m*,* 16.80H, CH2-CH2-CH2), 1.51 (m*, 2*.30H, CH2), 1.72 (m*, 2*.07H, CH2), 2.14 (*s,* 2.12H, CH3 ap), 2.17 (s, 2.22H, CH3 ap), 2.34 (t*, 2*.04H, NH-CO-CH2), 2.43 (2*s,* 2.66H, CH3 p), 2.71 (m*, 2*.00H, CH2-NH2), 6.85-7.70 (m, 6H, ArH), 8.18 (*s,* 0.32H, H-7 p), 8.22 (*s,* 0.52H, H-7 ap). [p:ap], conformers 38:62.

### Photochromic Polymers with Aromatic Amine PC

PMA (Sigma-531278, MW ~6,000; 18.0 mg, 3 µmol polymer, 120 µmol monomer) was added to a dry glass flask. $PCmNH_2$ (25.0 mg, 52 µmol) was dissolved in anhydrous THF (5.5 ml) and added to the PMA in the flask. The flask was sonicated for 2 min and left to react at 50 ºC with stirring. The solvent was reduced to approximately half and 5.55 mg of dodecylamine (30 µmol) was added to the flask and the reaction was left overnight at 60 ºC. An additional 11 mg (60 µmol) of dodecylamine was added and allowed to react for 6 h. A size-exclusion column of LH-20 suspended in $CHCl_3$ was utilized to separate unconjugated reagents. The final polymer PMA 6PC 75C12 was obtained as a dry film.

### Photochromic Polymers with Primary Amine PC

The ensuing methodology is for obtaining PMA 8PCaoc 75C12, the methodology is valid for the other polymers adjusting for the desired concentrations and linker length. Poly(isobutylene-*alt*-maleic anhydride (PMA, Sigma-531278, Mw ~6000, CAS: 26426-80-2; 6.0 mg, 1 µmol polymer, 40 µmol monomer) was added to a dry glass flask. PCaocNH2 (3.75 mg, 6 µmol) was prepared in anhydrous THF (1.0 ml) and added to the PMA in the flask. The flask was sonicated for 1 min and 2.8 mg (15 µmol) of dodecylamine was added and the reaction left overnight at 60 ºC. An additional 2.8 mg (15 µmol) of dodecylamine was added and allowed to react for 6 h. A size-exclusion column of Sephadex LH-20 (GE Healthcare) suspended in $CHCl_3$ was utilized to separate unconjugated reagents. After purification, 10 mg of dried polymer were obtained.

## References


1 Díaz, S. A., Giordano, L., Azcarate, J. C., Jovin, T. M. & Jares-Erijman, E. A. Quantum dots as templates for self-assembly of photoswitchable polymers: small, dual-color nanoparticles capable of facile photomodulation. *J. Am. Chem. Soc.* **135**, 3208-3217 (2013).

2 Efros, A. L. & Rosen, M. The electronic structure of semiconductor nanocrystals. *Annu. Rev. Mat. Sci.* **30**, 475-521 (2000).

3 van der Meer, B. W. Kappa-squared: from nuisance to new sense. *Rev. Molec. Biotechnol.* **82**, 181-196 (2002).

4 Díaz, S. A., Giordano, L., Jovin, T. M. & Jares-Erijman, E. A. Modulation of a photoswitchable dual-color quantum dot containing a photochromic FRET acceptor and an internal standard. *Nano Lett.* **12**, 3537-3544 (2012).